Holographic scattering in photopolymer-dispersed liquid crystals

M. A. Ellabban and M. Fally[a)]
Faculty of Physics, University of Vienna, Boltzmanngasse 5, A-1090 Vienna, Austria

H. Uršič
Faculty of Mathematics and Physics, University of Ljubljana, Jadranska 19, SI 1001, Ljubljana, Slovenia

I. Drevenšek-Olenik[b)]
Faculty of Mathematics and Physics, University of Ljubljana, Jadranska 19, SI 1001, Ljubljana, Slovenia and J. Stefan Institute, Jamova 39, SI 1001 Ljubljana, Slovenia

(Received 6 July 2005; accepted 15 August 2005; published online 3 October 2005)

Strong polarization-conserving holographic scattering was observed in a photopolymer-dispersed liquid crystal film fabricated from the UV curable mixture of commercially available constituents. During the photopolymerization process a bright corona of diffracted light evolves around the pump beam. The intensity of the rotationally symmetric light distribution increases upon exposure. By rotating the sample, two characteristic diffraction rings appear which can be explained by the Ewald sphere construction. Our results demonstrate that the associated parasitic holograms are very pronounced. Hence, their presence must be accounted for whenever preparing and utilizing holographic polymer-dispersed liquid crystals in any application. © *2005 American Institute of Physics*. [DOI: 10.1063/1.2089148]

Holographic polymer-dispersed liquid crystals (H-PDLCs) are holographic media that utilize photopolymerization induced phase separation to record three-dimensional optical images. They are composed of photosensitive monomers and liquid crystalline molecules. When exposing such a mixture to the optical field of two or more interfering laser beams, photopolymerization occurs more rapidly in bright than in dark regions of the interference pattern.[1,2] This leads to diffusion of liquid crystalline molecules into dark regions and of monomers to bright regions. Consequently, a periodic structure of alternating layers is formed, that is rich in polymer or of liquid crystal droplets, respectively. As a result, electrically switchable Bragg gratings with extremely high refractive-index contrast are achieved.[3,4] During the last decade it was demonstrated that H-PDLCs can be used for a broad range of applications such as low-power display devices, switches for telecommunications, integrated optical filters, photonic crystals, etc.[5–7] On the other hand, very little is known about optical imperfections of the H-PDLC structures. They are, however, very important as they determine the limits of the H-PDLC applicability in any realistic device. One of them is the evolution of unintentional photoinduced light scattering, known as holographic scattering (HS) in photorefractive media. This effect emerges from an initial scattering of the incident beam (pump beam) from inhomogeneities within the sample. The interference of the incident and scattered light produces a spatial modulation of intensity that is transferred to weak refractive-index gratings. Subsequently the pump beam is diffracted from these gratings. If the diffracted beam and the scattered beam are in phase, the latter will be amplified at the expense of the pump beam. This amplification process continues until certain limitations, e.g., pump beam depletion, lead to a steady state. Finally, a multitude of parasitic holograms (PHs) with different amplitudes and directions of grating vectors are recorded in the medium. As the PHs build up simultaneously with the desired primary hologram, they are also reconstructed at the same time. HS is a general phenomenon occurring in photosensitive materials. It is well known and basically understood in various acentric electro-optic crystals.[8–11] Further, it was observed a long time ago in photopolymers.[12] Only recently, HS was discovered also in centrosymmetric crystals, where amplification of the scattered light via two-beam coupling is forbidden by symmetry arguments.[13]

The HS process requires two necessary conditions to occur: an initial source of scattering and an effective amplification mechanism for the scattered light. Both of them are fulfilled in the H-PDLCs. Numerous liquid crystal droplets produced in the phase separation process represent intrinsic optical inhomogeneities within the structure, while a high refractive-index contrast between them and the surrounding polymer matrix results in a high diffraction efficiency of Bragg scattering. Consequently, light scattering from the droplets is expected to be strongly amplified.

In this letter we report on the observation of profound light-induced scattering in a transmission H-PDLC grating. Moreover, we characterize this effect in a photopolymerized PDLC structure made from the same initial mixture and prove that it can be classified as *holographic scattering*.

The samples were fabricated from a UV curable mixture prepared from commercially available constituents: a UV curable prepolymer (PN393, Nematel), nematic liquid crystal (TL203, Merck) and 1,1,1,3,3,3,3-Hexafluoroisopropyl acrylate (Sigma-Aldrich). The ratio of different constituents was selected following the formulations previously reported in literature.[14] A drop of the mixture was placed between two glass plates separated by 100 μm Mylar spacers. The samples were cured by irradiating them with an argon-ion laser at $\lambda_p = 351$ nm. Two different setups were used: In the single-beam recording setup the expanded laser beam penetrates the sample perpendicular to the surface. In the two-beam setup the beams entered the sample symmetrically with respect to the sample normal, i.e., a transmission grating

[a)]Electronic mail: martin.fally@univie.ac.at
[b)]Electronic mail: irena.drevensek@ijs.si

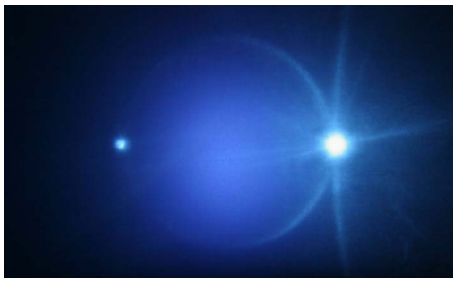

FIG. 1. (Color online) Far-field readout diffraction pattern of a H-PDLC fabricated from a 50/50 mixture of TL203 and PN393. The right spot is the transmitted beam and the left spot is the first-order diffracted beam. Bright rings with different diameters are related to holographic scattering. Recording and readout wavelength is 351 nm.

(with a grating pitch of 1 μm) was recorded. The total intensity of the writing beams was 9 mW/cm^2. During photopolymerization the temporal development of optical diffraction was monitored on a screen placed behind the sample and the far-field diffraction pattern was recorded by a digital camera. After the photopolymerization process the optical properties of the samples were analyzed by two He–Ne lasers at wavelengths $\lambda_{r1}=633$ and $\lambda_{r2}=543$ nm. The polarization of the probe and recording beams was the same. The typical power for readout was three orders of magnitude less than for recording in order not to destroy the holographic patterns. For the measurements of the transmitted intensity as a function of the readout angle, the samples were placed on a precise rotation stage and a Si photodiode was used to detect the intensity of the transmitted beam.

Figure 1 shows a far-field diffraction pattern of a single beam after having employed a conventional two-beam setup for preparing H-PDLC. The bright spot on the right side of the image corresponds to the transmitted beam, the less intense spot on the left side to the beam diffracted by the primary transmission grating. In addition, one can notice bright ring structures, that indicate the presence of HS.[15] These rings developed synchronously with the desired elementary grating.

To resolve the details of the corresponding scattering, we investigated these phenomena by using a single-beam recording setup. Figure 2 displays the intensity distribution of the far-field scattered light monitored at different times of the UV exposure. A corona of scattered light develops spatially symmetric around the transmitted beam. The diameter and the intensity of the corona increases with time. After an exposure of 0.23 Ws/cm^2 (26 s), the scattered light covers the whole screen size and a profound milky appearance of the sample can be noticed with the naked eye.

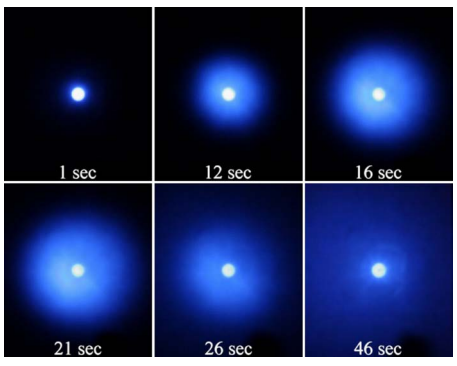

FIG. 2. (Color online) Far-field scattering patterns observed at different recording times of the UV beam, $\lambda_p=351$ nm and $I_p=9$ mW/cm^2. The central white spot corresponds to the transmitted beam.

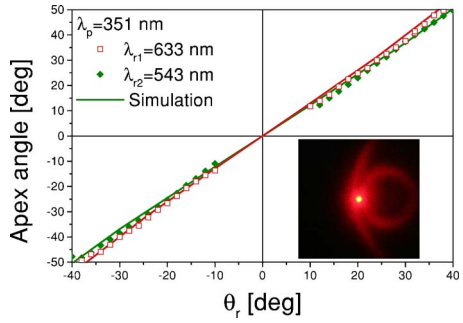

FIG. 3. (Color online) Measured and calculated apex angle of the conjugate image vs readout angle for $\lambda_{r1}=633$ and $\lambda_{r2}=543$ nm. Inset: far-field scattering pattern observed at $\theta_r=-14°$ using $\lambda_{r1}=633$ nm. The white spot corresponds to the transmitted beam.

Further analysis was focused on the samples cured for an exposure around 0.2 Ws/cm^2. Using a He–Ne we probed the diffraction patterns at different angles of the probe beam with respect to the sample normal. By rotating the sample, the symmetric corona of the scattered light transforms into two characteristic bright rings (Fig. 3). The diameter of these rings changes with the readout angle and the wavelength.

In 1974 Forshaw explained these ring patterns, that are characteristic for holographic scattering, in terms of the Ewald sphere construction.[15] The intersection of the Ewald sphere (allowed wave vectors of propagation in the medium) with the structure factor (primary and conjugate sphere[15,16]), i.e., the region in reciprocal space spanned by the recorded grating vectors, results in two cones. The projection of these cones on a screen then produces two bright rings. The apex angle of the cones derived from the Ewald-sphere construction is given by the following equation:

$$\xi = 2 \arctan\left[\frac{\sin \theta_r}{\cos \theta_r \pm \lambda_p/\lambda_r}\right], \tag{1}$$

where θ_r is the readout angle measured with respect to the normal incidence of the readout beam within the medium. The positive sign is assigned to the conjugate sphere, the negative sign to the primary sphere. For convenience we measured only the apex angle of the smaller ring—originating from the conjugate sphere—as a function of the readout angle. The results obtained for two different readout wavelengths are shown in Fig. 3. The solid lines in Fig. 3 represent simulations of Eq. (1) for the corresponding readout wavelengths. As can be seen, the experimental results are in good agreement with the theoretically predicted values. This proves that the phenomenon we are dealing with can be uniquely ascribed to polarization-conserving holographic scattering.

The angular selectivity of parasitic holograms at different readout wavelengths $\lambda_p \neq \lambda_r$ characterizes the spatial distribution of the light-induced refractive-index changes.[16,17] Therefore, we measured the transmitted intensity as a function of the readout angle. The corresponding results are shown in Fig. 4. It is clearly visible that the transmitted intensity increases with deviation from $\theta_r=0$. The reason is, that only in the case of readout conditions that are exactly the same as for recording, *all parasitic gratings simultaneously satisfy the Bragg condition* and give rise to low transmitted

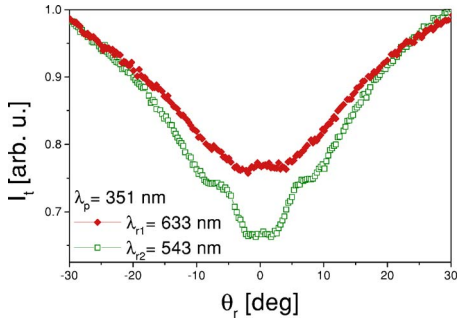

FIG. 4. (Color online) Transmitted intensity as a function of the readout angle for $\lambda_{r1}=633$ and $\lambda_{r2}=543$ nm.

intensity. Any deviation from the recording conditions, either in wavelength, angular position or polarization state,[18] increases the number of gratings for which the Bragg condition is violated and decreases the scattered intensity. For the experimentally chosen configuration with $\lambda_r \neq \lambda_p = 351$ nm, the transmitted intensity at $\theta_r = 0$ decreases to about 75% ($\lambda_{r1}=633$ nm) and 65% ($\lambda_{r2}=543$ nm).

In summary, the presence of HS in photosensitive H-PDLC and PDLC structures was evidently confirmed and characterized. Holographic scattering considerably reduces the light intensity and significantly corrupts the quality of holographic images recorded in these media. We anticipate that it is strongly present in practically all prepared H-PDLC structures. The reason that it was overlooked up till now might be attributed to the small thickness of the samples used for various investigations as compared to our experiment. Consequently, the sharpness of the characteristic conical diffraction patterns was also less. However, our investigation shows that HS is a prominent source of scattering and image blurring in H-PDLCs, and thus should be taken into account whenever preparing and using H-PDLC in any application.

The authors acknowledge the financial support of the ÖAD in the frame of STC program Slovenia-Austria (SI-A7/0405) and the Austrian Science Fund FWF (P-15642).

[1] C. C. Bowley and G. P. Crawford, Appl. Phys. Lett. **76**, 2235 (2000).
[2] T. Kyu, D. Nwabunma, and H.-W. Chiu, Phys. Rev. E **63**, 061802 (2001).
[3] R. L. Sutherland, V. P. Tondiglia, L. V. Natarajan, T. J. Bunning, and W. W. Adams, Appl. Phys. Lett. **64**, 1074 (1994).
[4] G. P. Crawford, Opt. Photonics News **14**, 54 (2003).
[5] V. P. Tondiglia, L. V. Natarajan, R. L. Sutherland, D. Tomlin, and T. J. Bunning, Adv. Mater. (Weinheim, Ger.) **14**, 187 (2002).
[6] R. L. Sutherland, V. P. Tondiglia, L. V. Natarajan, S. Chandra, D. Tomlin, and T. J. Bunning, Opt. Express **10**, 1074 (2002).
[7] M. J. Escuti, J. Qi, and G. P. Crawford, Appl. Phys. Lett. **83**, 1331 (2003).
[8] A. Ashkin, G. D. Boyd, J. M. Dziedzic, R. G. Smith, A. A. Ballman, A. A. Levinstein, and K. Nassau, Appl. Phys. Lett. **9**, 72 (1966).
[9] M. A. Ellabban, M. Fally, R. A. Rupp, T. Woike, and M. Imlau, in *Recent Research Development in Applied Physics* (Transworld, Trivandrum, India, 2001), Vol. 4, pp. 241–275.
[10] M. Goulkov, S. Odoulov, T. Woike, J. Imbrock, M. Imlau, E. Krätzig, C. Bäumer, and H. Hesse, Phys. Rev. B **65**, 195111 (2002).
[11] M. Goulkov, O. Fedorenko, L. Ivleva, M. Böttcher, T. Woike, T. Granzow, M. Imlau, and M. Wöhlecke, Phys. Rev. B **71**, 024104 (2005).
[12] J. M. Moran and I. P. Kaminow, Appl. Opt. **12**, 1964 (1973).
[13] M. Imlau, T. Woike, R. Schieder, and R. A. Rupp, Phys. Rev. Lett. **82**, 2860 (1999).
[14] I. Drevenšek-Olenik, M. Jazbinšek, M. E. Sousa, A. K. Fontecchio, G. P. Crawford, and M. Čopič, Phys. Rev. E **69**, 051703 (2004).
[15] M. R. B. Forshaw, Appl. Opt. **13**, 2 (1974).
[16] M. A. Ellabban, M. Fally, M. Imlau, T. Woike, R. A. Rupp, and T. Granzow, J. Appl. Phys. **96**, 6987 (2004).
[17] M. Imlau, M. Goulkov, M. Fally, and T. Woike, in *Polar Oxides: Properties, Characterization and Imaging*, edited by R. Waser, U. Böttger, and S. Tiedke (Wiley, New York, 2005), Chap. 9, pp. 163–188, ISBN: 3-527-40532-1.
[18] M. A. Ellabban, R. A. Rupp, and M. Fally, Appl. Phys. B: Lasers Opt. **72**, 635 (2001).